

The path towards mass manufacturing of optical waveguide combiners via large-area nanoimprinting

Matthias Jotz^{*1}, Frederik Bachhuber¹, Stefan Steiner², Brian Bilenberg³, Tobias Hedegaard Bro³, Jan Matthijs ter Meulen⁴, Erhan Ercan⁴, Janne Simonen⁵, Murat Deveci⁵
SCHOTT AG (Germany)¹, LightTrans International UG (Germany)², NIL Technology ApS (Denmark)³, Morphotonics B.V. (Netherlands)⁴, OptoFidelity Oy (Finland)⁵

ABSTRACT

A promising path towards consumer electronics-ready manufacturing of optical waveguide combiners is via large-area nanoimprinting surface relief gratings on an array of high index glass substrates. Presently, this is realized through equipment and substrates based on wafer formats (up to 12-inch). In this work, we present a way to produce waveguides with surface relief gratings utilizing the entire value chain from design to mastering to replication on panel-level nanoimprint equipment using rectangular high refractive index (RI) glass substrates and high refractive index resins. This is demonstrated on a greater than Gen 3 panel size (550 mm x 650 mm). The fabricated waveguides are optically tested to validate the design and the value chain. We demonstrate that the quality of the large area imprints is similar to present wafer-level imprints. Thus, we introduce a new approach towards high volume and low-cost manufacturing of waveguides based on surface relief gratings.

Keywords: metaverse, augmented reality, optical waveguides, nanoimprinting, optical design, mastering, high index glass, optical metrology

1. Introduction

Humans are highly visual creatures and interact most naturally with gadgets that present data in a visual format via displays. For the last 10-15 years, smartphones have exceedingly dominated our lives with ever-increasing resolutions for both the capture (camera) and display (screens) functions. In fact, since 2010, human eyes can no longer perceive individual pixels on a smartphone (below 300 microns).

Lately, the race for dominance between the smartphone makers has resulted in minor incremental changes, such as in the display resolution, causing consumers to upgrade their phones less frequently than before. Hence, there is an ongoing quest for the ‘next big thing’ that can replace smartphones altogether. The most common answer seems to be the ‘Augmented or Mixed Reality’ (AR or MR) smart glasses that have the potential to offer an as revolutionary leap as the ones from black and white to color TVs or landlines to mobile phones.

While designing and manufacturing universally accepted AR/MR smart glasses may still take many years to truly replace smartphones and sold in the billions, there is clearly a chicken-and-egg problem that requires bold moves and investments by technology companies to develop solutions to show that there is a path for commercially viable manufacturing of AR/MR smart glasses. In this paper, we focus on the technologically viable yet also commercially necessary and feasible manufacturing of the optical waveguide devices for AR/MR near-to-eye applications.

*matthias.jotz@schott.com

We have come together as a consortium of companies to showcase the manufacturing value chain from design to mastering to nanoimprinting to characterization by using the appropriate materials for large area manufacturing of optical waveguides with surface relief gratings, using a display-oriented manufacturing mindset, replicating on an array of glass substrates. Our goal was not to showcase the best performing, most efficient, smallest form factor AR optical waveguide solution. Instead, our common objective was to illustrate that such an end-to-end alternative manufacturing path is not only already accessible but is also much needed to meet the potential mass-market demand for cost-effective AR/MR optical waveguides.

2. Mass manufacturing of optical waveguide combiners via large-area nanoimprinting

2.1. Waveguide optics design by LightTrans International

For the general design approach of the demonstrator, a well-known and understood layout was chosen: A 1D-1D pupil expansion, which typically consists of three different grating regions (incoupler, exit pupil expander, and outcoupler, see Figure 1). As the name already implies, this particular approach is based on the separation of the dimensions of the pupil expansion in two different grating regions. While the uniform expansion of the pupil for the desired Field of View (FoV) and the transport of the light from incoupler to the demanded eye box are the main challenges of every waveguide design, in this approach the actual pupil expander grating is designed to multiply the beam in x-direction and the outcoupler likewise for the y-direction (see Figure 1). This separation of the pupil expansion allows for the utilization of 1D-periodic (so-called lamellar) grating structures for all mentioned grating regions, which enables a simpler design process and manufacturing as well. While this separation is the main advantage of this approach, the downside is a limited achievable maximum FoV, due to the increasing size of the expanding grating with a larger angular spectrum of the transported light.

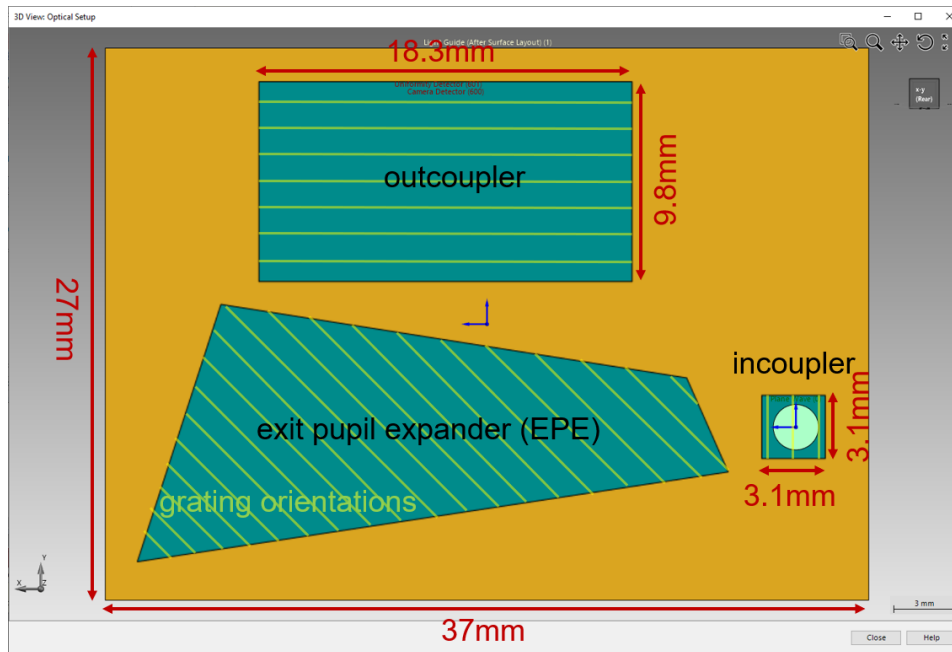


Figure 1: Top view of lateral layout of the designed waveguide. The orientations of the grating lines are indicated in green.

After choosing the general design approach, the lateral layout means, size and shapes of the grating regions can be calculated by geometrical considerations regarding the desired extent and position of the resulting eyebox. For this particular design task, the LightTrans International's physical-optics software "VirtualLab Fusion" was applied, which

provides versatile tools for the design and simulation of such layouts and other complex waveguide systems. In the following step, the required grating periods can be chosen according to the used wavelength, the refractive index of the substrate, and desired FoV. In this work, we are showing an exemplary design for 533 nm (with a gaussian spectrum and a bandwidth of 60nm) in combination with the desired FoV of $32^\circ \times 18^\circ$. Taking into account the refractive index of the utilized glass substrate at 533 nm (Schott RealView 1.9, thickness: $500\mu\text{m}$), the grating periods were designed to 415 nm for incoupler and outcoupler, and 293.45 nm for the expansion grating. The latter value already includes the rotation of the grating lines in the plane of the substrate surface of 45° . For choosing a proper lateral extent of the outcoupler the desired size of the eyebox ($15\text{mm} \times 8\text{mm}$) and eye relief (5mm) have to be considered (see Figure 1).

After setting proper sizes of all grating areas, the design of the actual grating structures is done. For the incoupler a blazed grating structure was chosen in order to enable a higher incouple efficiency of the intended diffraction order (T+1), due to the asymmetry of the structure. The expansion and outcouple grating were equipped with binary gratings, which provide a good trade-off between optical performance and feasible manufacturing. As for the grating material, a high refractive index resin was applied (Pixelligent PixNIL SFT1, $n=1.88 @ 533\text{nm}$), which almost matches the index of the substrate and assures appropriately performing gratings.

In order to achieve a suitable optical performance, which usually means a good lateral and angular uniformity in combination with an adequate efficiency of the whole device, the diffraction efficiency in EPE (Exit Pupil Expander) and outcoupler must be controlled via a lateral variation of the grating parameters. For this purpose, smooth modulations of grating height and ridge width (respectively fill factor) were introduced for EPE and outcoupler. Regarding the desired direction of pupil expansion for each grating region, the modulation was configured horizontally (x-direction) for the EPE and vertically (y-direction for the outcoupler (see Figure 2) with a linear slope. This linear and continuous modulation allows for a distinct reduction of the free parameters in the optimization, while not limiting the optical performance considerably.

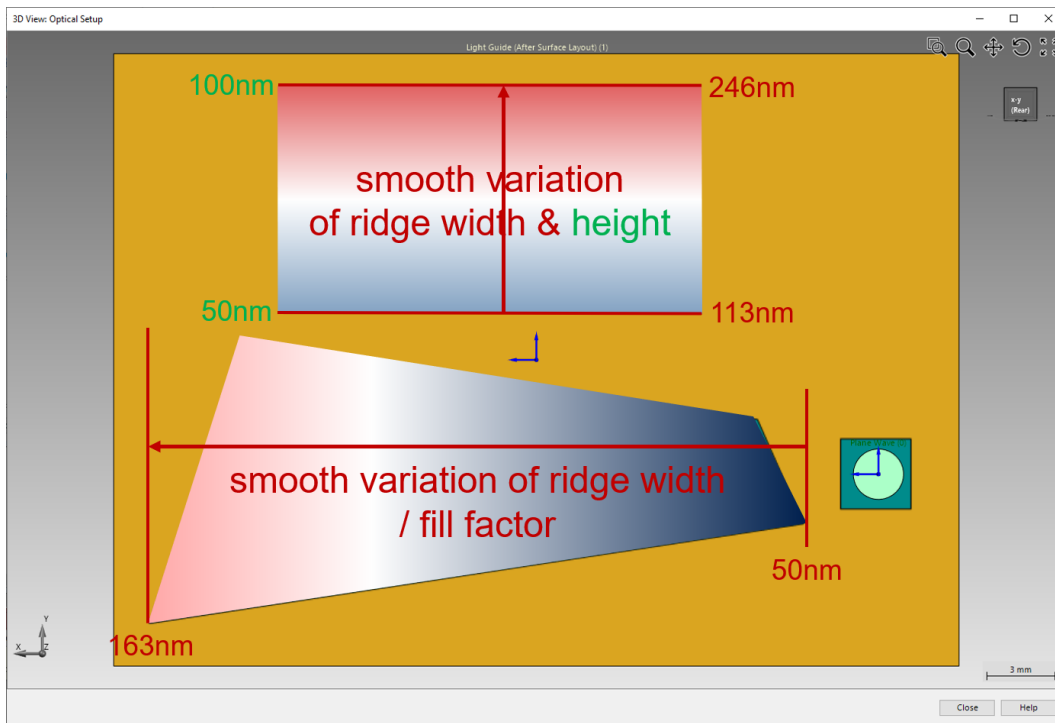


Figure 2: Depiction of modulation of grating parameters in EPE and outcoupler with results obtained by parametric optimization.

As the next step, parametric optimization was applied to find the best set of parameters. The following parameters were varied during this step: blaze angle of incoupler, height, and ridge width for EPE and outcoupler. As for the merit function, the lateral uniformity and efficiency were evaluated for 5 modes of the FoV (central mode and one of each FoV quadrant ($\pm 11^\circ, \pm 5^\circ$)). While the uniformity error should be as small as possible, the efficiencies of the different modes of the FoV are desired to be equal to provide a proper angular uniformity, as well. The design and optimization steps were done with VirtualLab Fusion, which enables a full physical optics analysis of such complex waveguide systems. Moreover, the diffraction efficiencies of the gratings are calculated rigorously by RCWA (Rigorous Coupled Wave Analysis), which also includes polarization effects during the light propagation inside the device. Due to the distinct sensitivity with respect to the polarization state of light for gratings in this range of structure size, the rigorous and local consideration for each individual interaction allows for very accurate modeling & design of the whole device.

Table 1: Overview of optimized grating parameters in the different regions of the designed waveguide.

	period	ridge width	height	blaze angle
incoupler	415 nm	415 nm (bottom)	203.1 nm	29.9°
pupil expander	293.45 nm	50 nm - 163 nm	50 nm	-
outcoupler	415 nm	113 nm - 263 nm	50 nm - 100 nm	-

The result of such optimizations usually exhibits a conflict between high efficiency and good uniformity, hence a design with good uniformity (mean uniformity error: 50.2%) and acceptable efficiency (mean efficiency per FOV mode: 0.8%) for the five FoV modes was chosen. The optimized grating parameters are shown in table 1.

The final simulation result of the optimized system for the central FOV mode can be found in Figure 3. The designed system exhibits a uniformity error of 46.0% and an efficiency of 2.0% for the central mode of the FOV. According to the chosen design approach of a 1D-1D pupil expander, these are adequate values. A higher performance would be achievable by exchanging the gratings in incoupler and outcoupler: Slanted grating profiles would offer more flexibility in the design, coming at a higher complexity during the fabrication.

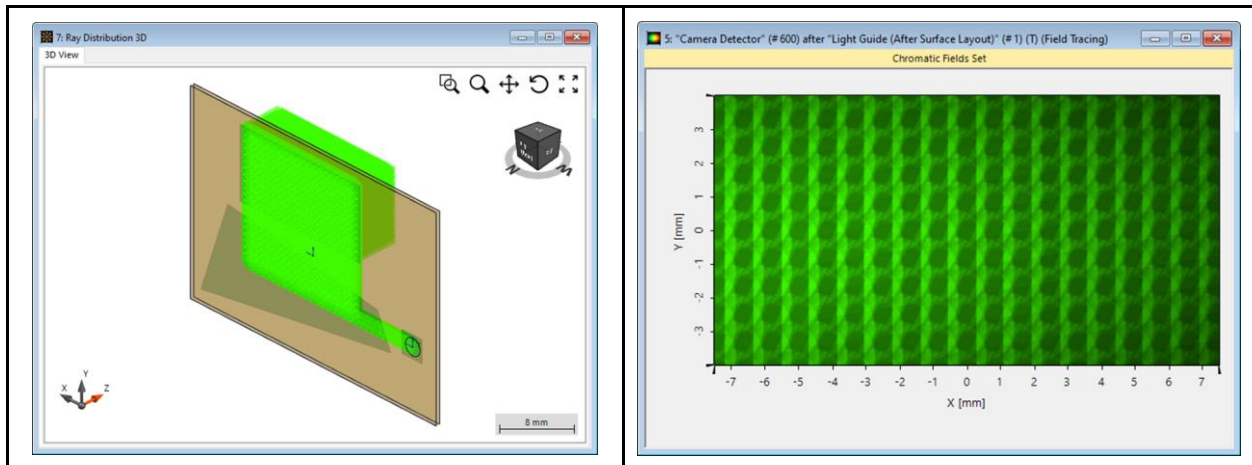


Figure 3: Left: Ray Tracing result of the designed waveguide for the central mode of the field of view (for illustration, just rays are shown, that hit the eyebox). Right: Field Tracing (physical optical) light distribution in the eyebox for the central mode (2.0% efficiency, 46.0% uniformity error).

2.2. Waveguide optics mastering by NIL Technology

The surface relief waveguide master is made in silicon by Electron Beam Lithography (EBL) and dry etching. This approach is chosen for the master fabrication to ensure the highest possible quality of the surface relief gratings. As detailed in Figure 4, a design with binary expander and output gratings and a blazed input grating was chosen to facilitate easy replication. The EBL is performed by a Jeol JBX-9500FSZ gaussian shaped 100 kV EBL tool in ZEP520A. For the blazed input grating a unique proprietary NIL Technology process is applied to ensure the highest possible quality of the blazed surfaces. The blazed grating period is defined with EBL and the blazed grating is formed by dry etching. The binary expander grating and the binary multi-depth output gratings are defined by EBL and etched by multiple ICP etching cycles with additional lithography steps in-between.

The use of EBL to define all gratings ensures a very high accuracy on the grating pitch and lateral dimensions. The use of dry etching to form the gratings in silicon ensures a high accuracy on the shape and etch depths. After pattern transfer, the master is cleaned and a first generation sub-master is generated by replication in Ormstamp on a glass wafer for subsequent recombination and fabrication of the waveguides.

In order to achieve the best performing waveguide designs, it is important to incorporate the design for manufacturing rules into the design process from the beginning which has been done in the work presented here. The choice of the design of the master presented in this work has been chosen to facilitate easy replication of the waveguide substrates. NIL Technology also offers more complex surface relief grating profiles like slanted gratings and shingles gratings and more advanced lateral patterns than line gratings. All these types of gratings can be combined on the master with total design freedom on relative placement and rotation of the individual gratings.

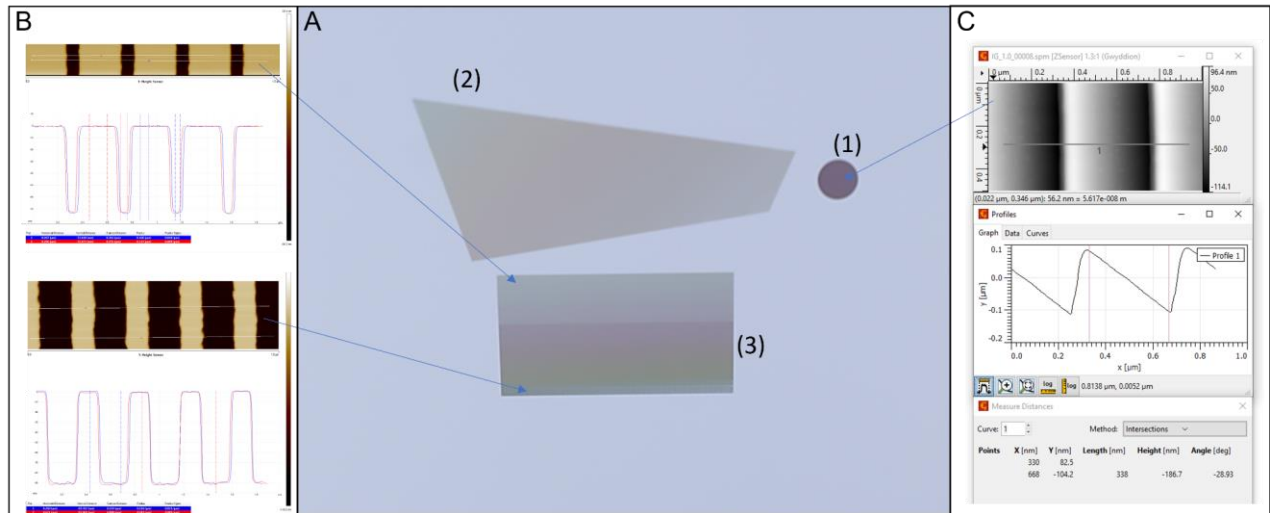


Figure 4. A: Complete AR master with blazed input grating (1), fill factor modulated expander grating (2) and depth and fill factor modulated output grating (3). B: AFM scans of Output grating showing both fill factor modulation from 17% (top) to 56% (bottom) and depth modulation from 72 nm (top) to 92 nm (bottom). C: AFM scan of blazed input grating showing the sharp profile with 29 degrees blaze angle.

2.3. Large area nanoimprinting of waveguides by Morphotonics

With the sub-master available, the next step is to replicate the surface relief waveguide optic component from the sub-master. To ensure mass manufacturing at high accuracy, the Roll-to-Plate (R2P) Nanoimprint Lithography (NIL) technology of Morphotonics has been used. The advantage of this imprint technology is that its scalability to larger substrate sizes, beyond wafer-scale, while maintaining good replication fidelity (preserved texture shape) and dimensional stability (no track pitch variation). Multiple rigid wafers can be imprinted in one pass, each containing a multiple-up of products adjacent to each other. Hereby, mass volume production is enabled.

The process starts with the scaling of the sub-master, containing one waveguiding eye-piece, to a scaled-up sub-master. With the Morphotonics proprietary upscaling process, an array of waveguiding eye-pieces is made. In this demo effort, the squared upscaled sub-master contains 6 rows of each having 5 eyepieces for a total of 30 eyepieces, as shown in Figure 5. Height variations between the different waveguiding products as well as the height and width of the seam in between the different waveguiding products have to be tightly controlled. Height variations result in a varying imprint pressure close to the seam. With the controlled Morphotonics' upscaling process the area next to the seam with deviations in imprint quality is minimized to a few mm. This small 'bleeding' area is outside the active area and is removed in the singulation of the eye-pieces.

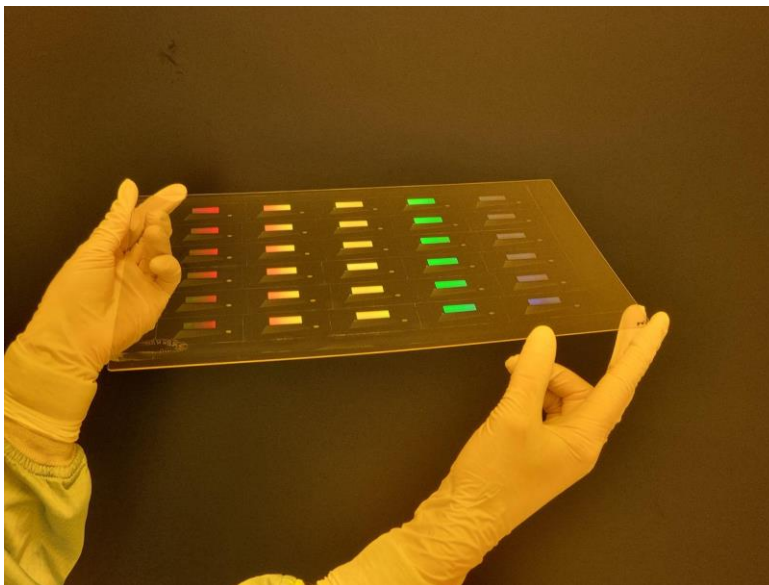


Figure 5. Imprint from the 30-up sub-master

The flexible stamp used in the large-area R2P imprint steps can contain multiple scaled-up sub-master areas, imprinting on multiple wafers placed on a carrier. In this demo work, the replication is made on a squared 300x300 mm wafer. With the use of the Morphotonics Portis NIL600 imprint module, handling up to 600 x 800 mm substrates, 4 wafers can be imprinted in one imprint cycle. The Morphotonics Portis NIL1100 can imprint up to a size of 1100 x 1300 mm, containing 9 wafers on a carrier. With 30 surface relief waveguiding optics on one wafer, 270 waveguiding components are made per imprint run. Typical TACT times (rate at which you need to complete a product) are around 6 minutes given the manual handling. In automated production, using the Morphotonics Aurora 1100 production line, the TACT can be reduced to 90 seconds, resulting in 10,800 imprints per hour or annually 90M eyepieces in 24/7 production.



Figure 6. Replication of the 30-up scaled-up sub-master on 4 single wafers in one imprint pass.

In the replication process, there are several key parameters: the re-usability of the flex stamp, the dimensional stability, the replication fidelity into resins with high refractive index and the layer thickness uniformity.

- The re-usability of the flexible stamp is important to ensure a reproducible process at lowest costs. With each imprint having the same imprint quality, limits the quality control step significantly. The Morphotonics flexible stamps have a re-usability of more than 500 times, proven in volume production with different customers.
- The track pitch of the different optical elements must remain constant within an imprint as well among different imprints. The flexible stamp is not allowed to be stretched due to the applied forces or thermal or humidity changes. To ensure this dimensional stability Morphotonics uses a High Dimensional Stability (HDS) stamp. This HDS flexible stamp is designed for its stability, having thermal expansion coefficients of 5 ppm/°C.
- A high refractive index resin has been used to match with the high refractive glass obtaining highest FOV. The solvent free resin has been co-developed and supplied by Pixelligent (Pixelligent PixNIL SFT1). The RI is 1.89 at a wavelength of 550 nm, with a viscosity of 575 CPs. The transmission of a 12 micron thick layer is over 94% with a very low haze. The refractive index of the PixNIL SFT1 has not yet been fine-tuned to the RI of the Schott glass.
- A uniform imprint, without variations in residual layer thickness, is required for best contrast and lowest waveguide losses. Lowest layer thickness variation is achieved with lowest residual layer thickness. The thickness of the residual layer is determined by the imprint process and resin characteristics. With the current solvent-free high-RI resin, a layer thickness of around 8 micron is obtained. Further development in solvent-free high-RI resin with lowered viscosity is needed to achieve minimal residual layer thicknesses.

The results in this paper arise from a combined effort of pioneering partners without time for optimization. The production chain has not been adjusted for deviations in the master process, sub-master up-scaling process or the different replication steps, nor have the materials used been fully optimized. As an example, the texture height has only been corrected by approximation for the shrinkage of the resin.

2.4. Waveguide glass materials by SCHOTT

Glass as a waveguide substrate material needs to ensure an efficient transmission of light within the boundary of the TIR (total internal reflection) condition. Hence, its material properties directly impact the performance of the waveguide. In addition to the obvious parameter of transmission there are two additional major parameters impacting waveguide quality. Firstly, the Refractive Index of the glass defines the TIR angle and therefore the achievable FoV (Field of View) of the waveguide. Secondly, the topology (TTV) of the glass surface influences the reflection angle locally and subsequently the clarity and MTF (Modular Transfer Function) of the transmitted image. For obvious reasons, cost is another important factor for the economic viability of an augmented reality headset.

The optical glass route:

In order to be able to produce optical glasses with high refractive index, not only the composition of the glass is of importance but also the melting technology. A complex set of redox reactions during the melting process need to be controlled in order to achieve the desired melting result. The higher the index, the harder it is to control the chemistry while melting. Then the liquid glass is poured into strips and coarse annealed. Afterwards the strips are fine annealed to achieve an exact match of the desired refractive index and eliminate any residual stress resulting in potential birefringence. Subsequently, the glass is wiresawn into raw wafer form. The raw wafers are then machined into their final outer shape and lapped and polished matching highest flatness standards.

This manufacturing route is the way optical glasses are being produced and brought into their final form. It is the route of choice because it offers a wide flexibility in melting process parameters, refractory materials and surface processing technology. However, this approach involves a significant amount of process steps and is limited in substrate dimensions by the cost of the required plano-plano processing especially when exceeding 12 inch wafer format.

The technical glass route:

For deliberately optimized glass types it is possible to use a continuous melting technology like Downdraw. In contrast to the optical glass route, the molten glass directly enters a hot-forming device in which the glass is drawn through a nozzle creating the flat, final and fire-polished surface. The resulting glass ribbon is then annealed, inspected and cut into sheets in-line. The sheets are then machined into wafer form.

Standard technical flat glasses like D263 or AF32 are produced in this manner. Due to its scalability and its near net shape forming capabilities, this route can be an interesting option for larger scale flat glass production in dimensions exceeding 12 inch wafer format. The relative ease in post processing speaks for itself. However, the hot forming process requires glass types that show a slow crystallization behavior, since for the forming to take place, the glass needs to retain a certain temperature over a period of time without losing its amorphous structure. This greatly limits the known glasses that are compatible with this process.

The path forward

Today's glass substrate based waveguides are usually based on glasses with a refractive index of around 1.8 and require a TTV of well below 1 μm on an 8 inch wafer. This can be achieved using the optical glass route. In order to show the potential of a rectangular, scalable flat glass for use as a waveguide substrate in the present demonstrator, we used our existing optical glass route and manufactured sheets sized 300x290 mm² out of our RealView 1.9 material.

In comparison to that, an advanced 8 inch wafer made via the technical glass route has a refractive index of around 1.5 and a TTV of smaller than 5 μm . It is obvious that there is a substantial gap in the current parameters using the technical route for waveguide substrates. The reason for this gap is, that the glasses' tendency to crystallize rises with higher refractive

index, which represents a physical obstacle in hot forming as explained above. In addition, the production of an extremely low TTV in hot forming is also challenging due to the complexity and the large scale machinery involved. However, we see a path on our roadmaps to improve on both, refractive index and TTV, using the technical route.

Summary

Putting into relation the three main factors impacting waveguides (TTV, refractive index and cost) we end up with two antagonizing approaches towards a glass substrate for waveguide use. A first one focusing on quality, delivering highest refractive index and best surface topology (TTV) and a second one circling around cost while economizing the quality parameters as mentioned before. Even though there is still a gap between the two manufacturing approaches, the gap can substantially be narrowed by further development of material and process. However, this requires substantial development effort, which can most likely only be justified in future generations of AR headsets.

2.5. Waveguide optics metrology by OptoFidelity

We investigated the quality of the replicated samples with two complementary measurement methods, image quality measurement and Littrow diffractometer.

For the end user of an AR device, the image quality produced by the projector and the waveguide is naturally the most important part of the user experience. Typical pico-projectors used in commercial headsets are not the best choice for characterizing the waveguides, as they typically lack the stability, uniformity and/or contrast required for accurate metrology. In this case we assembled a laboratory reference projector. It is based on green LED Köhler illumination to achieve uniform illumination of a checkerboard reticle. The full-field reticle pattern is then projected to infinity with an eyepiece, which also creates the exit pupil with adjustable exit pupil size, to match the input grating of the sample. The reticles can be changed to assess different waveguide parameters, but in these first tests we concentrated on checkerboard measurements, as it allows measuring not only contrast but also luminance non-uniformity.

To characterize the image we used OptoFidelity OptoEye 1.0 lens with a grayscale machine vision camera. The lens is designed with an external entrance pupil, which can be placed to the eyebox of the waveguide. The field of view is 100 deg diagonal, allowing seeing the full image from the waveguide without tilting the camera. Projecting the full-field image is a standard way to assess waveguide image quality. An alternative is to do traditional MTF-measurements at selected angles but this does not give any information on for example luminance non-uniformity, which is often a critical parameter for diffractive waveguides.

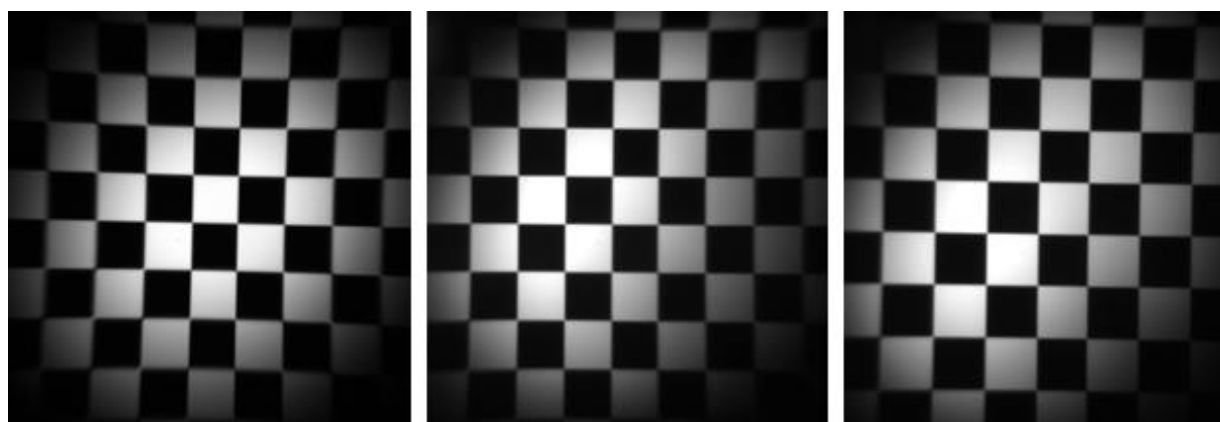


Figure 7. Image quality measurements from the first batch of samples. Reference image directly on the projector (left), images from the eyebox of samples 1 and 2, (middle and right, respectively). The field-of-view of the image is approximately 22 x 22 degrees.

In the images from Figure 7, you can see the measurement results of the first two replicated samples. The reference image was first taken directly from the projector, by matching the entrance pupil of the camera lens with the exit pupil of the projector. Usually in waveguide image quality testing the projector image luminance will be adjusted to be as uniform as possible, but due to time constraints this was not possible, and the image is very vignetted at the corners of the 22 x 22 degree field of view. However, for qualitative assessment of the replication process this is not a problem, as we just need to visually compare the reference image with the images taken from the eyebox of the samples.

For the waveguides, the input grating was placed on the exit pupil of the projector and the camera into the eyebox at the eye relief distance of 5 mm. The results are seen in the figure 7. Typically, the largest challenge for diffractive waveguides is luminance uniformity, but here the images from the samples are nearly identical to the reference image. This is a very good result as the fabrication process had not yet been optimized in any way.

We analyzed the checkerboard contrast from the images by comparing the center white square average pixel value to the average of the surrounding black squares. The dark current of the camera sensor was naturally subtracted first. The reference contrast from the projector in this case was about 1:90, and for the samples about 1:26. Compared to the best waveguides on the market that can reach a contrast of around 1:100 the result leaves much room for improvement, but this is likely largely explained by sub-optimal contrast of the projector. Our projector designs can easily exceed the contrast of 1:300, but as mentioned, in this case we did not have time to optimize the projector performance for these samples.

Image quality is typically an excellent metric for assessing AR waveguide quality. However, if image quality is not satisfactory, it can be challenging to figure out why. We used a Littrow diffractometer to measure the uniformity of the grating period and also the relative angles of the grating lines in all the grating areas. Properly built and calibrated, Littrow diffractometers can reach accuracies in the picometer and arcsecond range for those parameters. For the gratings to optimally function, these extreme accuracies are actually necessary.

The goal of a Littrow diffractometer is relatively simple, to measure the Littrow angle of a grating as accurately as possible. In our system we have a very stable and narrow bandwidth solid state laser at 405 nm wavelength. The beam quality is improved with a spatial filter - a pinhole and a pair of lenses. The collimated beam then illuminates a spot on the sample, which is placed on a stack of two Aerotech rotary stages to control yaw and roll. The stages are rotated until the laser diffracts exactly back to the laser. This is observed with a machine vision camera through a beamsplitter placed in front of the laser.

When the Littrow condition is reached, the grating period can be calculated from the sample yaw stage position and the diffraction equation. The grating lines will be vertical, so the roll stage directly gives the relative grating angle. The measurements can be repeated for different spots on the sample as the laser is placed on an xy-stage. As a spot-by-spot measurement the method is inherently quite time-consuming, especially for non-uniform gratings, as it takes time to see anything on the small field-of-view camera sensor. Therefore it is typically used in investigating masters before replication and then sampling the produced replicas, as well as investigating samples that have failed the image quality test.

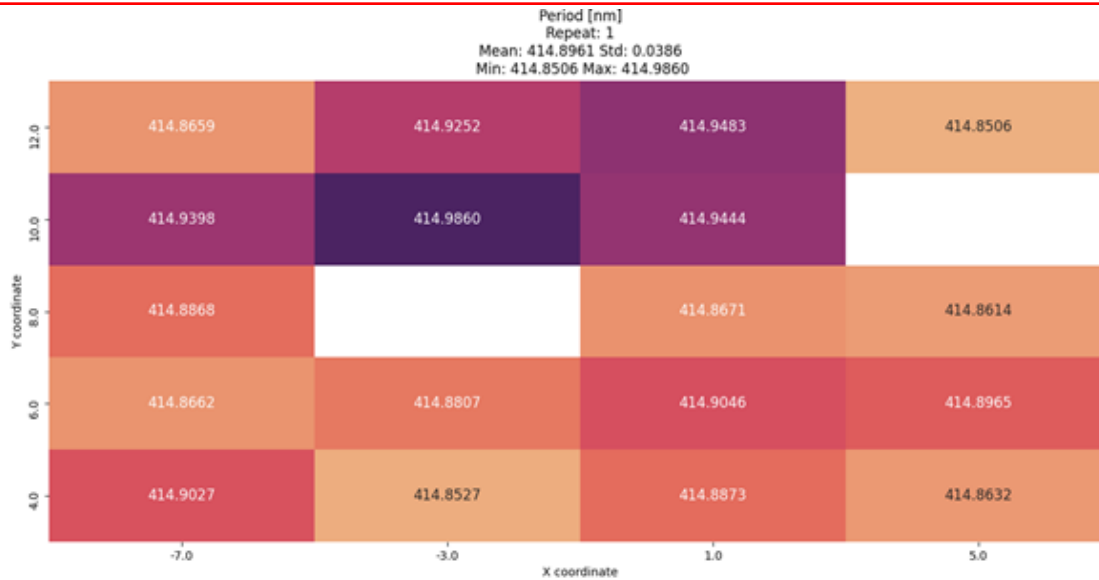


Figure 8. Grating period uniformity for Sample 3-6, grating 3 (output). 20 points were measured in a 2 mm grid. Two points could not be measured, likely due to local surface defects. The period was 414.90 +/- 39 pm.

As an example of the results, we measured the input and output gratings of Sample 3-6. The designed grating period was 415 nm for both of them, and they should be at exactly 90 deg orientation compared to each other. We measured the average periods to be 414.98 nm and 414.90 nm for gratings 1 and 3, respectively. The uniformity for grating 3 is depicted above, with the one sigma standard deviation being +/- 40 pm. This is an excellent result, demonstrating the high quality of the whole manufacturing chain. The average relative orientation was 89.99973 degrees, which corresponds to an orientation error of 1.0 arc seconds. As this is already below the repeatability of the lab setup used in the measurements, the samples also show very high quality with regards to relative grating orientation.

3. Conclusions

Will the high-volume manufacturing of AR waveguide optics help trigger the ubiquitous adoption of Smart glasses, making them the ‘next big thing’ and helping to pave the way towards the ‘metaverse’? Time will tell how quickly the industry will take the necessary steps towards this objective.

In the interim, we have demonstrated in this paper that for a successful transition to high-volume manufacturing of AR waveguide optics, a display-oriented, large-area manufacturing mindset is not only needed, but is also already available. The array of high-quality squared glass enables the increase in production volume of AR waveguide optics. Together with the complex design, the high-end master and the in-depth quality inspection capabilities available, the large-area R2P NIL imprinted demo proves that the mass production route is feasible.

Finally, an end-to-end supply chain and cooperation between different disciplines is also key. As a consortium of pioneers, we were able to show good waveguiding at first pass with a robust design, excellent mastering, using unprecedented materials and proven large-area nanoimprinting, topped with the unique metrology capabilities. We hope this exemplary work will inspire the industry to take the necessary steps to help fulfill the promise of Smart glasses.

Acknowledgments

The authors would like to thank their colleagues for their support of this work.